Eur. Phys. J. C 48, 457–466 (2006)
DOI 10.1140/epjc/s10052-006-0050-4

THE EUROPEAN PHYSICAL JOURNAL C

Regular Article – Theoretical Physics

Truncated first moment of the parton distribution – A modified approach

D. Kotlorz[1,a], A. Kotlorz[2,b]

[1] Opole University of Technology, Division of Physics, Ozimska 75, 45-370 Opole, Poland
[2] Opole University of Technology, Division of Mathematics, Luboszycka 3, 45-036 Opole, Poland

Received: 7 May 2006 / Revised version: 30 August 2006 /
Published online: 24 October 2006 – © Springer-Verlag / Società Italiana di Fisica 2006

Abstract. We derive the LO DGLAP evolution equation for the full Mellin moments of the first moment of the nonsinglet parton distribution truncated at x_0. This "moment of moment" approach allows one to determine the small-x_0 behaviour of the truncated first moment. We compare our predictions to results obtained from x-space solutions for parton distributions with use of the Chebyshev-polynomial method and to solutions of the evolution equations for the truncated moments proposed by other authors. The comparison is performed for different input parametrisations for $10^{-5} \leq x_0 \leq 0.1$ and $1 \leq Q^2 \leq 100\,\mathrm{GeV}^2$. We give an example of an application to the determination of the contribution to the Bjorken sum rule.

PACS. 12.38.Bx; 11.55.Hx

1 Introduction

Deep inelastic scattering (DIS) experiments provide knowledge about the internal structure of the nucleon. Measurements on proton, deuteron and neutron targets allow also for the verification of sum rules [1–3] – basic relations in QCD. Sum rules for unpolarised and polarised structure functions refer to their Mellin moments. Particularly important roles in the experimental and theoretical QCD tests play the first moments of the parton densities, which have a physical interpretation and can be determined from the data. From an experimental point of view, however, the accurate verification of sum rules is unreliable. Determination of the sum rules requires knowledge of the structure functions over the entire region of the Bjorken variable $x \in (0;1)$. The lowest limit of x in the present experiments is about 10^{-5} and the limit $x \to 0$, which means that the invariant energy W^2 of the inelastic lepton-hadron scattering becoming infinite ($W^2 = Q^2(1/x - 1)$) will never be attained. Therefore it is very hopeful in the theoretical analysis to deal with truncated instead of full moments of the structure functions. This enables one to avoid uncertainties from the unmeasurable $x \to 0$ region. The most familiar theoretical approach, which describes scaling violations of the parton densities in perturbative QCD has been formulated by Dokshitzer, Gribov, Lipatov, Altarelli and Parisi (DGLAP) [4–7]. The evolution equations for the moments of parton distributions truncated at low x_0 are however more complicated than in a case of the full moments. These are not diagonal and each nth truncated moment couples to the $(n+j)$th ($j \geq 0$) truncated moments [8–10]. For $n \geq 2$ the series of couplings to higher moments is very fast convergent. Even for a small ($m = 4$) number of terms in the expansion of the truncated counterpart of the anomalous dimension G_n, the higher moments can be calculated with excellent accuracy. The first moment is more sensitive to the truncated point x_0 and the convergence of G_n for $n = 1$ is weaker than for the higher moments. Nevertheless, it has been shown in [11] that for more terms of the G_n expansion ($m \sim 30$) the uncertainty in the determination of the first moment at $x_0 \leq 0.1$ and $Q^2 = 10\,\mathrm{GeV}^2$ does not exceed 5% independent on the input parametrisation. However, this increase with m of the accuracy does not proceed infinitely. Numerical errors, which occur for larger m (dependent on x_0) make further improvement of the precision impossible. It may be very useful to discuss the methods of the theoretical determination of truncated first moments of parton distributions, because these predictions would be directly verified experimentally. In this paper we present an approach in which we compute the first moments truncated at small x_0 using the inverse Mellin transform of their full moments. In other words, our method is based on the solutions for the full nth moments of the truncated first moment of the parton distribution. This "moment of moment" technique would be complementary to other

[a] e-mail: dstrozik@po.opole.pl
[b] e-mail: kotlorz@po.opole.pl

known methods in the determination of the sum rule contributions.

The content of this paper is as follows. In Sect. 2 we recall the ways of computing the truncated moments within the DGLAP approximation. Thus Sect. 2.1 contains a brief description of the Chebyshev-polynomial approach for x-space solutions of the DGLAP evolution equations. In Sect. 2.2 we recall the idea of the DGLAP evolution equation for the truncated moments, which underlies our "moment of moment" technique. This modified method is presented in Sect. 2.3. For simplicity we consider the quark nonsinglet LO evolution. In Sect. 3 we compare solutions for the first moment of the nonsinglet structure function truncated at small x_0, obtained with use of the above-mentioned earlier approaches. As an example we explore the Bjorken sum rule (BSR). In Sect. 4 we present predictions for the low-x contribution to the BSR together with experimental constraints. Finally, in Sect. 5 we summarise our results.

2 Determination of the truncated Mellin moments of parton distributions

For the (full) Mellin moments of the parton distributions $p(x,Q^2)$ we have

$$M[p](n,Q^2) = \int\limits_0^1 \mathrm{d}x x^{n-1} p(x,Q^2)\,; \tag{1}$$

for these the DGLAP evolution equation can be solved analytically. This is because in the moment space n one obtains simple diagonalised differential equations. The only problem is the knowledge of the input parametrisation for the whole region $0 \le x \le 1$, which is necessary in the determination of the initial moments $M[p](n, Q^2 = Q_0^2)$:

$$M[p]\left(n,Q_0^2\right) = \int\limits_0^1 \mathrm{d}x x^{n-1} p\left(x,Q_0^2\right)\,. \tag{2}$$

Using the truncated moments approach one can avoid the uncertainties from the region $x \to 0$, which will never be attained experimentally.

The Mellin moment of the parton distribution $p(x,Q^2)$ truncated at x_0 is defined by

$$M[p]\left(x_0,n,Q^2\right) = \int\limits_{x_0}^1 \mathrm{d}x x^{n-1} p(x,Q^2)\,. \tag{3}$$

From the theoretical point of view, there are two ways to avoid the problem of dealing with the unphysical region $x \to 0$. The first one is to work in x-space and obtain directly the evolution of the parton distributions (not of their moments). The best known methods for solving the Q^2 evolution equations for parton distributions in x-space are the brute-force [12], Laguerre-polynomial [13, 14] or Chebyshev-polynomial [15–18] approaches. In this way, the truncated moment can be simply found by integrating the x-space solutions $p(x,Q^2)$ over the cut range $x_0 \le x \le 1$ (see Sect. 2.1). An alternative way is to use the evolution equations directly for the truncated moments. The appropriate DGLAP evolution equations for the truncated moments have been derived in [8–10]. Authors have shown that these equations, though not diagonal, can be solved with quite good precision for $n \ge 2$, even for a very small number of terms in the expansion series. In the case of the first moment, the accuracy is worse and more terms in the G_n expansion must be taken into account. We briefly recall the idea of solving the evolution equations for truncated moments in Sect. 2.2. Based on this idea, we have derived the evolution equation for a truncated first moment in a diagonal form. The appropriate integro-differential equation contains only one function – $q_1(x,Q^2)$, which denotes the first moment truncated at x, without coupling to the other, higher moments. Then, using the full Mellin moments approach, we have found the small-$x = x_0$ behaviour of the function $q_1(x,Q^2)$, which is simply the first moment truncated at low-x_0. A detailed description is given in Sect. 2.3.

2.1 LO DGLAP evolution equations with use of the Chebyshev-polynomial expansion

The Chebyshev-polynomial technique [19] was successfully used by Kwieciński in many QCD treatments [15–18]. Using this method one obtains a system of linear differential equations instead of the original integro-differential ones. For example, in order to solve the LO DGLAP evolution equation for the nonsinglet parton distribution $p \equiv q^{\mathrm{NS}}$,

$$\frac{\partial p(x,t)}{\partial t} = \frac{\alpha_{\mathrm{s}}(t)}{2\pi} \int\limits_x^1 \frac{\mathrm{d}z}{z} P_{qq}\left(\frac{x}{z}\right) p(z,t)\,, \tag{4}$$

one has to expand the functions $p(x,t)$ into the series of the Chebyshev-polynomials. In this way, the integration over z in the evolution equation (4) can be performed, which leads to the system of linear differential equations

$$\frac{\mathrm{d}p(x_i,t)}{\mathrm{d}t} = \sum_{j=0}^{N-1} H_{ij} p(x_j,t)\,. \tag{5}$$

This system can be solved by using the standard Runge–Kutta method with initial conditions given by the input parametrisation $p(x_j,t_0)$. The moments truncated at x_0 are simply computed numerically via integrating (3). The Chebyshev expansion provides a robust method of discretising a continuous problem. This allows for computing the parton distributions for a "not too singular" input parametrisation in the whole $x \in (0;1)$ region. A more detailed description of the Chebyshev-polynomial method in solving the QCD evolution equations is given e.g. in the appendix of [11].

2.2 Evolution equations for truncated moments

LO DGLAP evolution equation for the Mellin moment of the nonsinglet structure function truncated at x_0 found by Forte, Magnea, Piccione and Ridolfi (FMPR) [8–10] has the form

$$\frac{\partial M[p](x_0,n,t)}{\partial t} = \frac{\alpha_{\rm s}(t)}{2\pi}\int\limits_{x_0}^{1} {\rm d}y y^{n-1} p(y,t) G_n\left(\frac{x_0}{y}\right) , \quad (6)$$

where

$$t \equiv \ln\frac{Q^2}{\Lambda^2_{\rm QCD}} , \quad (7)$$

and

$$G_n(z) \equiv \int\limits_{z}^{1} {\rm d}y y^{n-1} P_{qq}(y) \quad (8)$$

is the truncated anomalous dimension. Expanding $G_n(x_0/y)$ into a Taylor series around $y=1$ gives

$$\frac{\partial M[p](x_0,n,t)}{\partial t} = \frac{\alpha_{\rm s}(t)}{2\pi}\sum_{j=0}^{m} C_{jn}^{(m)}(x_0) M[p](x_0,n+j,t) . \quad (9)$$

Equation (9) is not diagonal, but each nth moment couples only with $(n+j)$th $(j\geq 0)$ moments. Because the series of couplings to the higher moments is convergent, and furthermore the value of the $(n+j)$th moments decreases rapidly in comparison to the nth moment, one can retain from (9) the closed system of $m+1$ equations:

$$\frac{\partial M[p](x_0,n,t)}{\partial t} = \frac{\alpha_{\rm s}(t)}{2\pi}\sum_{j=n}^{N_0+m} D_{nj}^{(N_0+m-n)}(x_0) M[p](x_0,j,t) . \quad (10)$$

Here

$$N_0 \leq n \leq N_0+m , \quad (11)$$

where N_0 is the lowest considered moment and D is a triangular matrix. The solution of (10) has the form

$$M[p](x_0,n,t) = \sum_{k=n+1}^{N_0+m} A_{nk}(x_0) M[p](x_0,k,t) + \left(M[p](x_0,n,t_0) - \sum_{k=n+1}^{N_0+m} A_{nk}(x_0) M[p](x_0,k,t_0)\right) \times \exp\left(c_f D_{nn}^{(m)}(x_0)\ln\frac{t}{t_0}\right) . \quad (12)$$

The matrix elements $D_{ij}^{(m)}(x_0)$ and $A_{ij}(x_0)$ are given in [8–11]. In [11] the results (12) have been compared to those obtained with the use of the Chebyshev-polynomial technique. The agreement of both approaches is excellent for higher moments $(n\geq 2)$ and not too large $x_0 \leq 0.1$, even for a small number of terms $(m=4)$ in the truncated series (12). It also does not depend strongly on the scale Q^2 or the input parametrisation. In the case of a truncated first moment, a similar accuracy requires more terms $(m\geq 30)$ to be taken into account.

In the next section we estimate the small-x_0 behaviour of the truncated first moment $M[p](x_0,n=1,t)$.

2.3 Small-x_0 behaviour of the truncated first moment

We would like to present a possible way of an approximate determination of the small-x_0 behaviour of the truncated first moment $M[p](x_0,1,t)$. Our starting point is the evolution equation (6), which for the first moment has the form

$$\frac{\partial q_1(x_0,t)}{\partial t} = \frac{\alpha_{\rm s}(t)}{2\pi}\int\limits_{x_0}^{1} {\rm d}y p(y,t) G_1\left(\frac{x_0}{y}\right) . \quad (13)$$

Here we denote in short-hand the truncated first moment by $q_1(x_0,t)$:

$$q_j(x_0,t) \equiv M[p](x_0,j,Q^2) . \quad (14)$$

Inserting $G_1(z)$ in the LO approximation,

$$G_1(z) = \frac{8}{3}\ln(1-z) + \frac{4}{3}\left(z+\frac{z^2}{2}\right) , \quad (15)$$

we obtain

$$\frac{\partial q_1(x_0,t)}{\partial t} = \frac{2\alpha_{\rm s}(t)}{3\pi} \times \left[x_0 q_0(x_0,t) + \frac{x_0^2}{2} q_{-1}(x_0,t) - 2\sum_{k=1}^{\infty}\frac{x_0^k}{k} q_{1-k}(x_0,t)\right] . \quad (16)$$

In the above formula we have used the expansion of $\ln(1-z)$:

$$\ln(1-z) = -\sum_{k=1}^{\infty}\frac{z^k}{k} . \quad (17)$$

Taking into account that

$$q_j(x_0,t) = x_0^{j-1} q_1(x_0,t) + (j-1)\int\limits_{x_0}^{1} {\rm d}y y^{j-2} q_1(y,t) , \quad (18)$$

we find

$$\frac{\partial q_1(x_0,t)}{\partial t} = \frac{2\alpha_{\rm s}(t)}{3\pi}\left[q_1(x_0,t)\left(\frac{3}{2} - 2\sum_{k=1}^{\infty}\frac{1}{k}\right) + \int\limits_{x_0}^{1}{\rm d}y \left(2\sum_{k=1}^{\infty}\frac{x_0^k}{y^{k+1}} - \frac{x_0}{y^2} - \frac{x_0^2}{y^3}\right) q_1(y,t)\right] . \quad (19)$$

The above result is the LO DGLAP evolution equation for the truncated first moment of the nonsinglet parton distribution. This formula contains only q_1 and there is no mixing of q_1 and higher or lower moments q_j. Therefore we can adopt for (19) the well known approach and write the evolution equation of q_1 in the moment space, which reads as follows:

$$\frac{\partial M[q_1](n,t)}{\partial t} = \frac{2\alpha_s(t)}{3\pi} H(n) M[q_1](n,t)\,. \tag{20}$$

$H(n)$ is given by

$$H(n) = 2\sum_{k=1}^{\infty}\left(\frac{1}{n+k}-\frac{1}{k}\right)+\frac{3}{2}-\frac{1}{n+1}-\frac{1}{n+2}\,. \tag{21}$$

In this "moment of moment" approach (MM) we have obtained a simple equation for a some complicated structure $M[q_1](n,t)$, which is the (full) nth moment of the truncated first moment of the parton density, namely

$$M[q_1](n,t) = \int_0^1 \mathrm{d}x x^{n-1} \int_x^1 \mathrm{d}y p(y,t)\,. \tag{22}$$

The solution of (20) is

$$M[q_1](n,t) = M[q_1](n,t_0)\exp[a(t)H(n)]\,, \tag{23}$$

where $M[q_1](n,t_0)$ is the initial value of $M[q_1]$ for the low scale t_0:

$$M[q_1](n,t_0) = \int_0^1 \mathrm{d}x x^{n-1} \int_x^1 \mathrm{d}y p(y,t_0) \tag{24}$$

and

$$a(t) = \frac{8}{33-2N_f}\ln\frac{t}{t_0}\,, \tag{25}$$

with N_f the number of the quark flavours. Hence $q_1(x,t)$ is given by the inverse Mellin transform

$$q_1(x,t) = \frac{1}{2\pi\mathrm{i}}\int_{c-\mathrm{i}\infty}^{c+\mathrm{i}\infty} \mathrm{d}n x^{-n} M[q_1](n,t_0)\exp[a(t)H(n)]\,. \tag{26}$$

The behaviour of $q_1(x,t)$ for $x\to 0$ is governed by the leading (i.e. rightmost) singularities of $M[q_1](n,t_0)$ as well as $H(n)$ in the n complex plane [20]. If we parametrise the input parton distribution $p(x,t_0)$ in the general form

$$p(x,t_0) \sim x^{a_1}(1-x)^{a_2}\,, \tag{27}$$

we obtain

$$M[q_1](n,t_0) \sim \frac{1}{n}\beta(a_1+1,a_2+1) - \sum_{k=0}^{k_{\max}} \frac{(-1)^k}{k!}\frac{\Gamma(a_2+1)}{\Gamma(a_2+1-k)(a_1+1+k)(n+a_1+1+k)}\,. \tag{28}$$

$\Gamma(z)$, $\beta(z_1,z_2)$ in (28) are Euler functions and $k_{\max}$ depends on a_2 in the following way:

$$k_{\max} = \begin{cases} \infty & \text{for fractional } a_2 > 0\,, \\ a_2 & \text{for whole } a_2 \geq 0\,. \end{cases} \tag{29}$$

One can see from (21) and (28) that $H(n)$ has the rightmost pole at $n=-1$, while $M[q_1](n,t_0)$ at $n=0$ and $n=-a_1-1$. In this way, for the shape of the starting distribution nonsingular at small x, $p(x,t_0)$ ($a_1=0$), the simple pole at $n=0$ and the essential singularity at $n=-1$ are the leading ones. Then the small-x_0 behaviour of the truncated first moment can be determined by the method of steepest descent. We find

$$q_1(x,t) \approx \frac{1}{a_2+1} - \sqrt{\frac{e}{2\pi}}\beta(a_2+1,z)x_0 z^{1.5}[z+2a(t)]^{-0.5} \times \exp\left(a(t)H(z-1)+0.5\sqrt{1-4a(t)\ln(x_0)}\right)\,, \tag{30}$$

where

$$z \equiv -\frac{1+\sqrt{1-4a(t)\ln(x_0)}}{2\ln(x_0)}\,. \tag{31}$$

If we consider a more singular input parametrisation $p(x,t_0)$ ($a_1<0$), this singular small-x behaviour remains stable against the LO Q^2 QCD evolution. In this case the approximate behaviour of the truncated first moment $q_1(x,t)$ is governed by the leading simple poles of $M[q_1](n,t_0)$, situated at $n=0$ and $n=-a_1-1$:

$$q_1(x,t) \approx \beta(a_1+1,a_2+1) - \sum_{k=0}^{k_{\max}} \frac{(-1)^k}{k!}\frac{\Gamma(a_2+1)x^{a_1+1+k}}{\Gamma(a_2+1-k)(a_1+1+k)} \times \exp[a(t)H(-a_1-1-k)]\,. \tag{32}$$

In the next section we compare the results (30)–(32) with those obtained within approaches described in Sect. 2.1 and Sect. 2.2.

3 Results for the truncated first moment within three different approaches

In this section we present numerical results for the truncated first moment of the nonsinglet parton distribution. Predictions obtained with the use of different methods are denoted via CHEB, FMPR or MM, according to the applied approach (see Sects. 2.1–2.3 respectively). Thus $q_1^{\mathrm{CHEB}}(x_0,t)$ results from integrating

$$q_1^{\mathrm{CHEB}}(x_0,t) = \int_{x_0}^1 \mathrm{d}x x^{n-1} p^{\mathrm{CHEB}}(x,t)\,, \tag{33}$$

where $p^{\mathrm{CHEB}}(x,t)$ is the solution of (4) and (5), while

$q_1^{\mathrm{FMPR}}(x_0,t)$ is implied by (12) and has the form

$$q_1^{\mathrm{FMPR}}(x_0,t) = \sum_{k=2}^{m+1} A_{1k}(x_0) q_k(x_0,t) + \left(q_1(x_0,t_0) - \sum_{k=2}^{m+1} A_{1k}(x_0) q_k(x_0,t_0) \right) \times \exp\left(c_f D_{11}^{(m)}(x_0) \ln \frac{t}{t_0} \right) , \qquad (34)$$

where $q_k(x_0,t)$ is defined by (14).

The analytical approximate solutions (30)–(32), describing the low-x_0 behaviour of $q_1(x_0,t)$ within the "moment of moment" (q_1^{MM}) approach are compared with the q_1^{CHEB} and q_1^{FMPR} results in Figs. 1–6. We consider two values of the number of terms in the truncated series for the FMPR-m predictions ($m=4$, $m=30$). We show the results for the first moment of g_1^{NS} truncated at x_0, which is a contribution to the Bjorken sum rule [2, 3]. In the figures

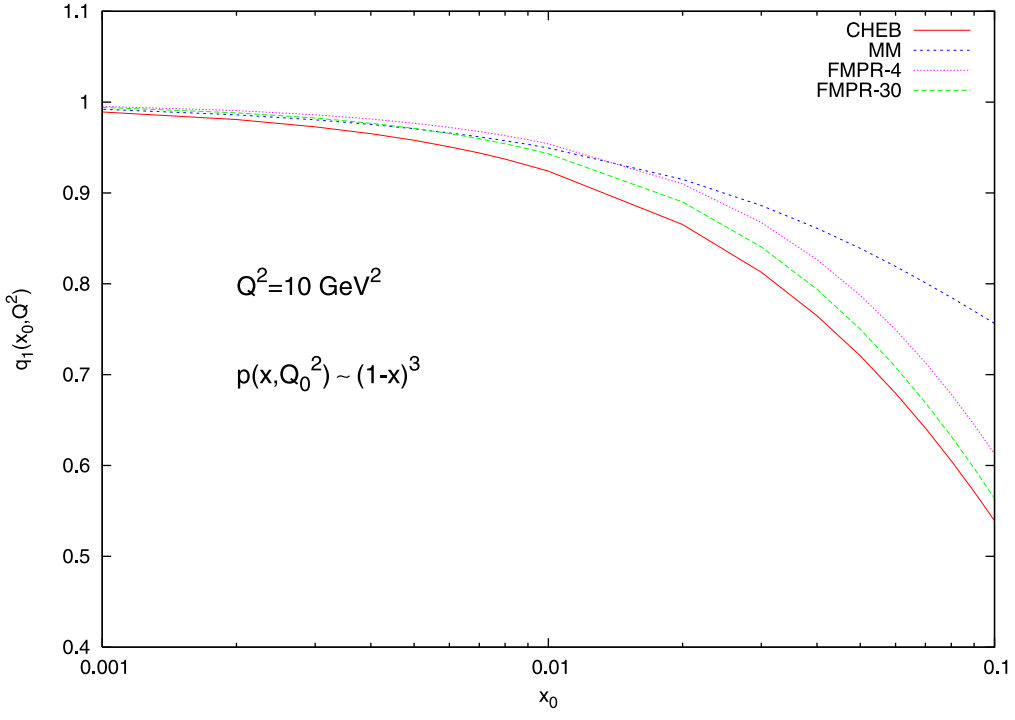

Fig. 1. Small-x_0 behaviour of the truncated at x_0 first moment of the nonsinglet spin structure function g_1^{NS} in the case of the flat input (35). A comparison of (30) (MM) with the predictions based on the Chebyshev-polynomial method (CHEB) and FMPR approach (34) for two values of the number of terms in the truncated series, $m=4$, $m=30$, are shown. The Bjorken sum rule is normalised to 1

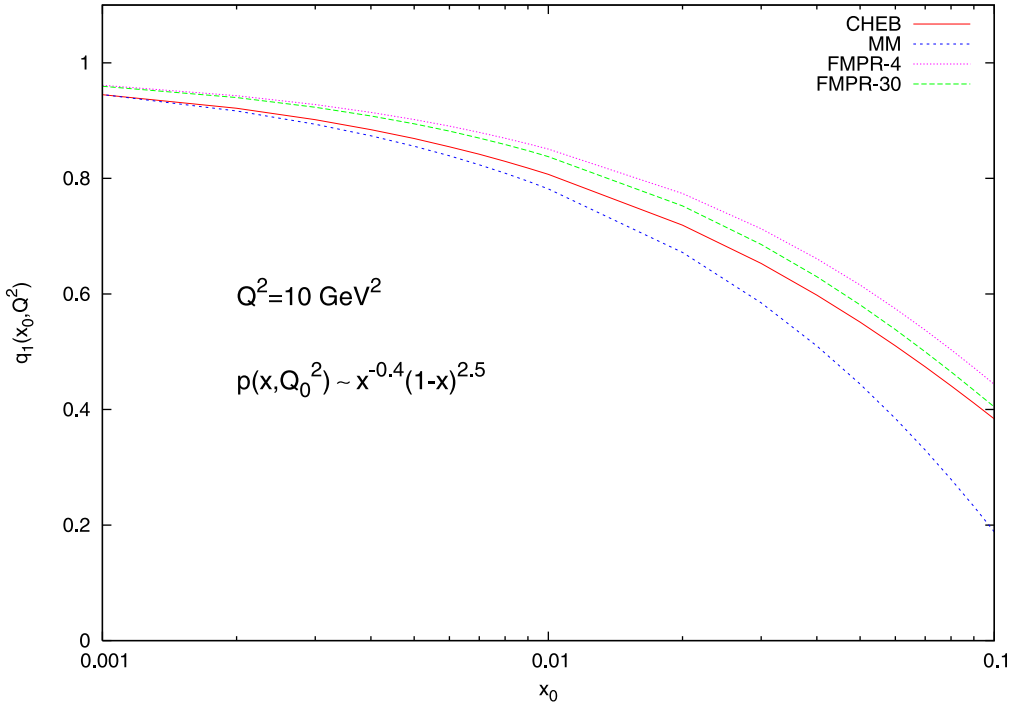

Fig. 2. Small-x_0 behaviour of the first moment of the nonsinglet spin structure function g_1^{NS} truncated at x_0 in the case of the steep input (36). A comparison of (32) (MM) with the predictions based on the Chebyshev-polynomial method (CHEB) and FMPR approach (34) for two values of the number of terms in the truncated series, $m=4$, $m=30$, are shown. The Bjorken sum rule is normalised to 1

presented the total Bjorken sum rule is normalised to 1. We use two different inputs at $Q_0^2 = 1\,\mathrm{GeV}^2$, namely

$$p\left(x, Q_0^2\right) \equiv g_1^{\mathrm{NS}}\left(x, Q_0^2\right) \sim (1-x)^3\,, \tag{35}$$

$$p\left(x, Q_0^2\right) \equiv g_1^{\mathrm{NS}}\left(x, Q_0^2\right) \sim x^{-0.4}(1-x)^{2.5}\,. \tag{36}$$

A parametrisation (36) more singular at small x incorporates the latest knowledge about the low-x behaviour of the polarised structure functions [21, 22]. The integral $\int \mathrm{d}x g_1^{\mathrm{NS}}$ truncated at $x_0 = 0.01$ is reduced by about 8% for the Regge input (35) and about 20% for (36) in comparison to the total Bjorken sum rule. Figures 1–6 show that for small $x_0 \leq 0.01$ there is a good agreement between the MM results (30)–(32) and the predictions obtained with the use of the Chebyshev-polynomial approach, which can be regarded as reliable. The percentage

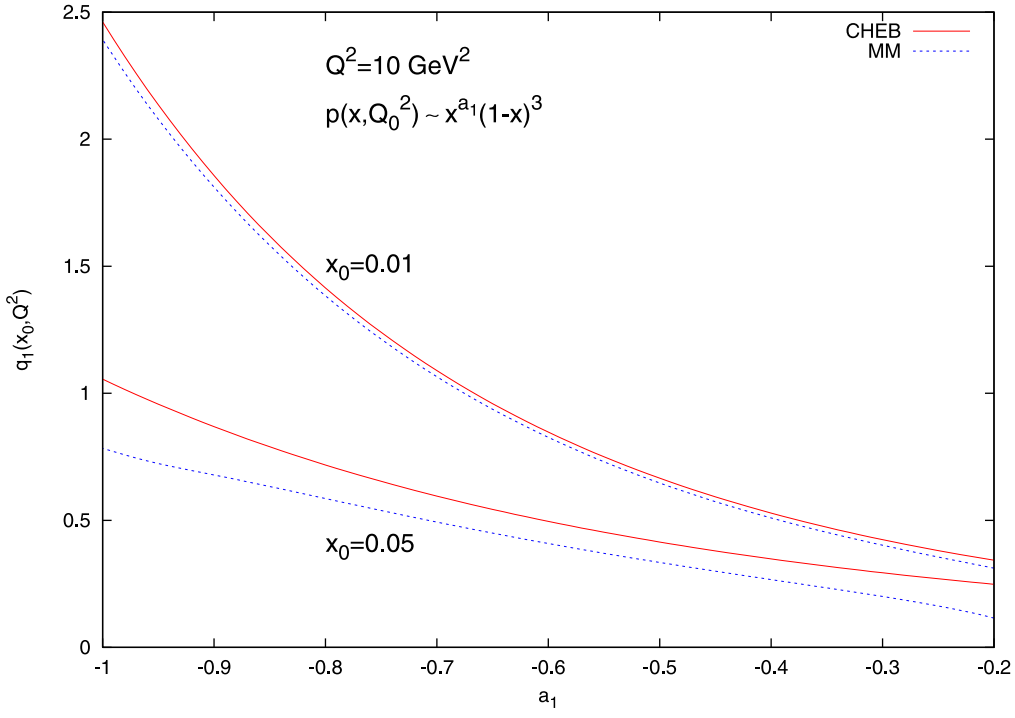

Fig. 3. Truncated first moment q_1^{MM} (32) as a function of a_1 in the input parametrisation $p(x, Q_0^2) \sim x^{a_1}(1-x)^3$ for fixed $x_0 = 0.01$ and $x_0 = 0.05$. A comparison with the predictions based on the Chebyshev-polynomial method is shown

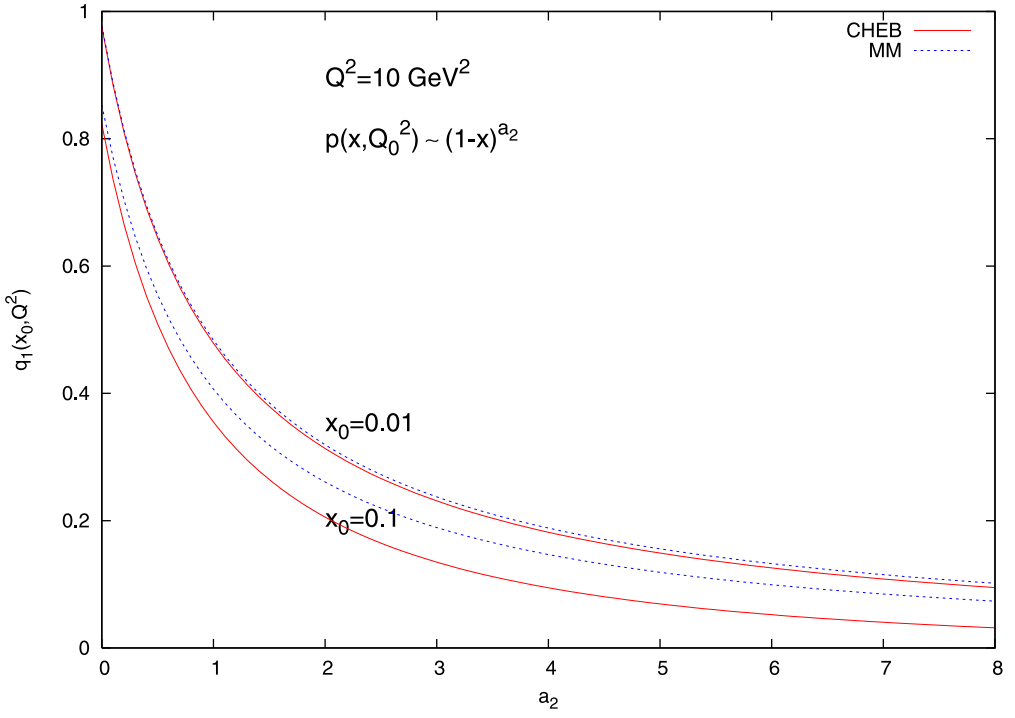

Fig. 4. Truncated first moment q_1^{MM} (30) as a function of a_2 in the input parametrisation $p(x, Q_0^2) \sim (1-x)^{a_2}$ for fixed $x_0 = 0.01$ and $x_0 = 0.1$. A comparison with the predictions based on the Chebyshev-polynomial method is shown

error

$$E^a(x_0,Q^2)=\frac{\left|q_1^a(x_0,Q^2)-q_1^{\mathrm{CHEB}}(x_0,Q^2)\right|}{q_1^{\mathrm{CHEB}}(x_0,Q^2)}\cdot 100\%\,, \quad (37)$$

where a denotes MM, FMPR-4 or FMPR-30 results, is about 3% in the case of MM solutions for $x_0=0.01$ and $Q^2=10\,\mathrm{GeV}^2$, independent on the shape of the input parametrisation. A similar accuracy gives taking into account more terms ($m=30$) in the truncated series within the FMPR approach (FMPR-30), while for $m=4$ the error (37) is about 4% in the case of the flat input and 6% in the case of the more singular one. $E^a(x_0,Q^2)$ grows slowly with increasing Q^2 (see Figs. 5 and 6) and for $Q^2=100\,\mathrm{GeV}^2$ we get $E^{\mathrm{MM}}(x_0=0.01,Q^2)\approx E^{\mathrm{FMPR\text{-}30}}(x_0=0.01,Q^2)\approx 4\%$ for the flat parametri-

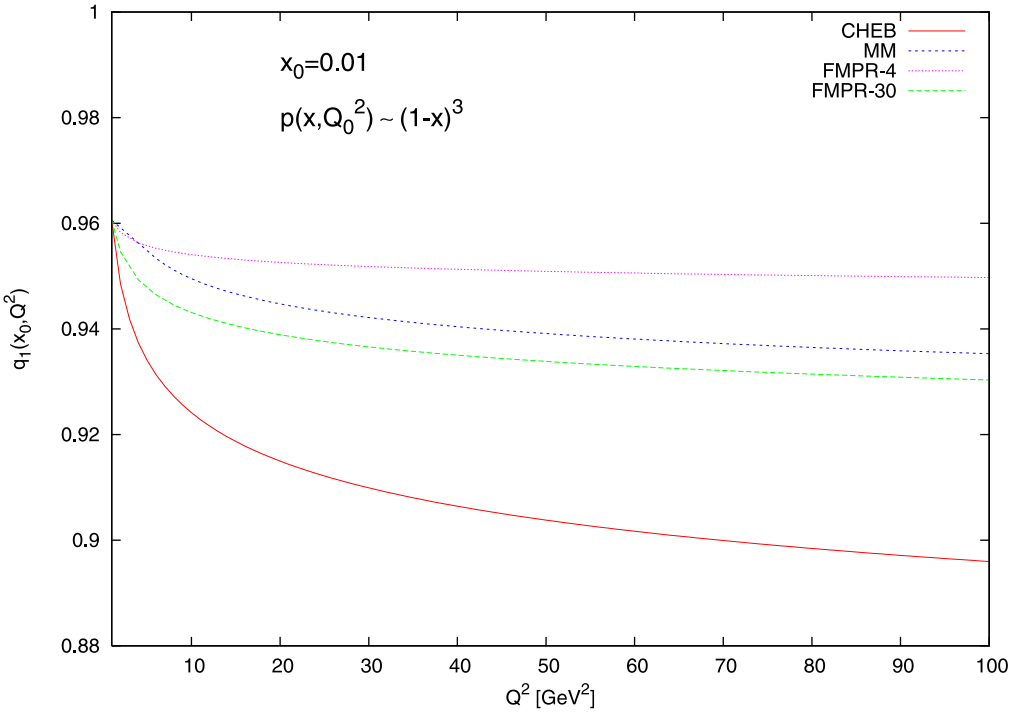

Fig. 5. Q^2 dependence of the truncated first moment q_1^{MM} (30) at fixed $x_0=0.01$ for input parametrisation (35). A comparison to the predictions based on the Chebyshev-polynomial method and FMPR approach (34) for two values of the number of terms in the truncated series, $m=4$, $m=30$, is shown

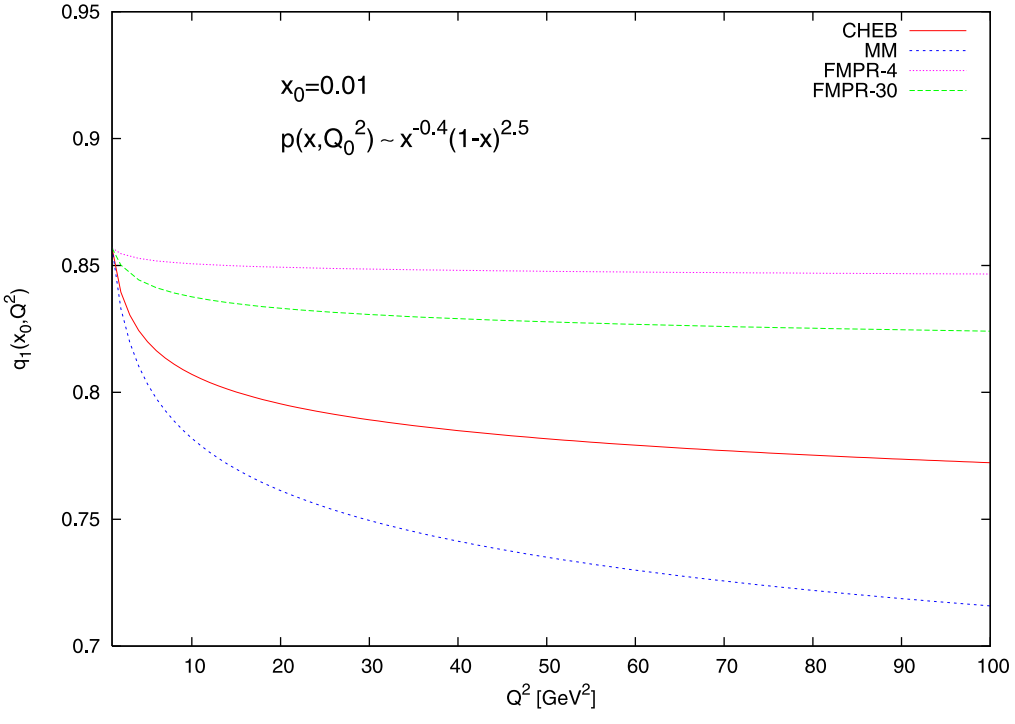

Fig. 6. Q^2 dependence of the truncated first moment q_1^{MM} (32) at fixed $x_0=0.01$ for input parametrisation (36). A comparison to the predictions based on the Chebyshev-polynomial method and FMPR approach (34) for two values of the number of terms in the truncated series, $m=4$, $m=30$, is shown

sation and 7% respectively for the more singular input. Note that for the truncation points $x_0 \leq 0.01$ our approximate analytical solutions (30)–(32) are as reliable as the FMPR-30 predictions and more exact than the FMPR-4 results. This does not depend either on the shape of the input parametrisation or on the value of Q^2.

In the next section we determine the low-x contribution to the Bjorken sum rule.

4 Low-x contribution to the Bjorken sum rule

Among all moments of the structure functions, the Bjorken sum rule (BSR) [2, 3] is one of the convenient tests of QCD. BSR is a fundamental relation for polarised scattering, describing a relationship between spin dependent DIS and the weak coupling constant defined in neutron β-decay. In the limit of the infinite momentum transfer Q^2, the BSR reads

$$I_{\mathrm{BSR}} \equiv \Gamma_1^p - \Gamma_1^n = \int_0^1 \mathrm{d}x \left(g_1^p(x) - g_1^n(x)\right) = \frac{1}{6}\frac{g_\mathrm{A}}{g_\mathrm{V}}\,, \quad (38)$$

where g_V and g_A are the vector and axial vector couplings. From recent measurements [23] $g_\mathrm{A}/g_\mathrm{V} = 1.2695 \pm 0.0029$. BSR refers to the first moment of the nonsinglet spin dependent structure function g_1^{NS}:

$$g_1^{\mathrm{NS}}(x, Q^2) = g_1^p(x, Q^2) - g_1^n(x, Q^2)\,, \quad (39)$$

where g_1^p and g_1^n are the spin structure functions for the proton and neutron. The asymptotic relation (38) at finite $Q^2 \gg \Lambda^2_{\mathrm{QCD}}$ takes the form, with pQCD corrections,

$$\int_0^1 \mathrm{d}x g_1^{\mathrm{NS}}(x, Q^2) = \frac{1}{6}\frac{g_\mathrm{A}}{g_\mathrm{V}}\left[1 - \frac{\alpha_\mathrm{s}}{\pi} - 3.583\left(\frac{\alpha_\mathrm{s}}{\pi}\right)^2 - 20.215\left(\frac{\alpha_\mathrm{s}}{\pi}\right)^3\right]. \quad (40)$$

The validity of the sum rule is confirmed in polarised DIS at the level of 10% [24–28]. Evaluation of the sum rules requires knowledge of the polarised structure functions over the entire region of x: $0 \leq x \leq 1$. The experimentally accessible x range for the spin dependent DIS is however limited ($0.7 > x > 0.003$ for the SMC data [24–26], $0.6 > x > 0.023$ for the HERMES data [29–31]), and therefore one should extrapolate the results to $x = 0$ and $x = 1$. The extrapolation to $x \to 0$, where the structure functions grow strongly, is much more important than that to $x \to 1$, where the structure functions vanish. The extrapolation towards $x = 0$ suffers from large uncertainties, being essentially dependent on the used QCD fit. The "flexibility" of the chosen parametrisation appears in the agreement with the experimental data, giving however enough freedom in the unmeasured regions [32]. In the case of the BSR this allows for a significant reduction of the low-x contribution.

In our approach we can test how the small-x contribution to the BSR depends on the different (less steep or steeper) input parametrisations at the initial scale $Q_0^2 = \mathrm{GeV}^2$:

$$g_1^{\mathrm{NS}}\left(x, Q_0^2\right) = \eta x^{a_1}(1-x)^{a_2}\,. \quad (41)$$

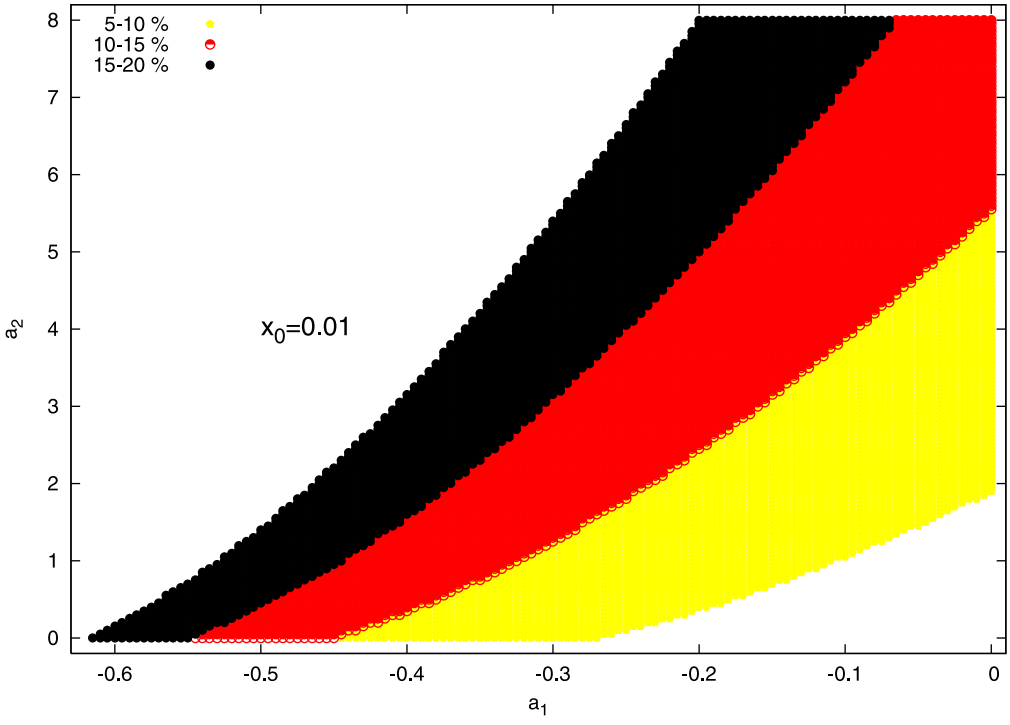

Fig. 7. Low-x contribution to the Bjorken sum rule (43) for different a_1 and a_2 in the input parametrisation (41). $x_0 = 0.01$ and $Q^2 = 5\,\mathrm{GeV}^2$

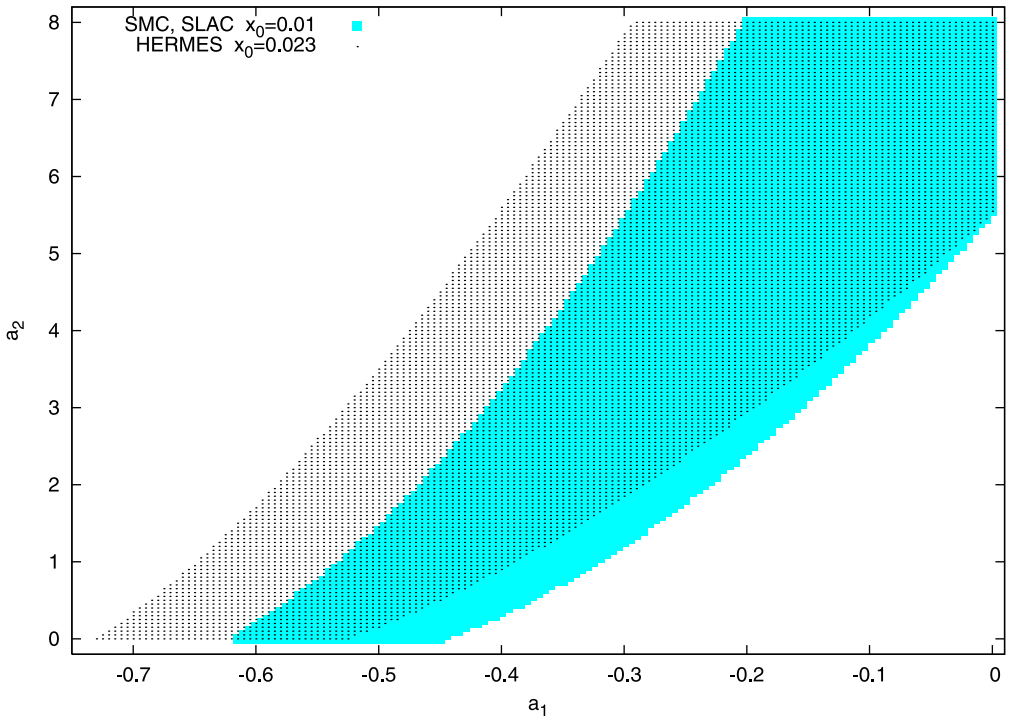

Fig. 8. Constraints on the parametrisation of $g_1^{\rm NS}$, implied by the experimental estimations of the low-x contribution to the Bjorken sum rule. SMC, SLAC: $10\% \le r(x_0 = 0.01, 5) \le 20\%$ (full colour), HERMES: $20\% \le r(x_0 = 0.023, 5) \le 40\%$ (*dotted*)

Here η is a normalization factor:

$$\eta = \frac{I_{\rm BSR}}{\beta(a_1+1, a_2+1)}\,. \tag{42}$$

The exponent a_1 controls the behaviour of the structure function $g_1^{\rm NS}$ as $x \to 0$ and the factor $(1-x)^{a_2}$ ensures the vanishing of $g_1^{\rm NS}$ at $x \to 1$. The percentage contribution to the BSR, coming from the small-x region $0 \le x \le x_0$ is defined by

$$r\left(x_0, Q^2\right) = \frac{\int\limits_0^{x_0} {\rm d}x g_1^{\rm NS}(x, Q^2)}{\int\limits_0^1 {\rm d}x g_1^{\rm NS}(x, Q^2)} \cdot 100\%\,. \tag{43}$$

The ratio r for $x_0 = 0.01$ varies from a few to tens of percents for the different configurations of $-1 \le a_1 \le 0$ and $0 \le a_2 \le 8$. The r-distribution at $x_0 = 0.01$ is shown in Fig. 7. One can see that the small-x contribution to the BSR grows with increasing a_2 and decreasing a_1. For the Regge flat parametrisation (35) r is at the level of 5–10%, what is significantly different from the result based on the input (36), where $r \sim 20\%$. From theoretical analyses it is known that the small-x behaviour of the nonsinglet polarised structure function g_1^{NS} is governed by the double logarithmic terms i.e. $(\alpha_{\rm s} \ln^2 x)^n$ [21, 22, 33–35]. This leads to the form of $g_1^{\rm NS}$ singular at low-x

$$g_1^{\rm NS}(x, Q^2) \sim x^{-\lambda}\,, \tag{44}$$

with $\lambda \approx 0.4$. The LO DGLAP approach with use of the singular input (36) pretends the double logarithmic $\ln^2 x$ resummation. Low-x experimental data [24–26, 29–31] clearly confirm the rise of $g_1^{\rm NS}$ in this region. However, the errors on the present data are too large to reliably support or contradict this $x^{-0.4}$ behaviour. The "freedom" in the initial parametrisation to satisfy the small-x experimental extrapolation of the BSR is seen in Fig. 8. The experimental data can be satisfactorily reproduced by e.g. input $\sim (1-x)^6$ nonsingular as $x \to 0$ and by e.g. the singular one, $\sim x^{-0.5}(1-x)^1$, as well. SMC and SLAC measurements imply that 10–20% of the BSR comes from x values less than 0.01 [24–28, 36]. Also the HERMES data [29–31] enable one to determine the low-x contribution to the BSR at 0.023 between 20–40%. The wide range of these estimations could be restricted by new spin data concerning this mystery and the small-x region of interest.

5 Conclusions

In this paper we have compared results for the first moment q_1 of the parton distribution truncated at x_0 obtained within different approaches. Thus we have solved numerically the LO DGLAP evolution equation for the nonsinglet function in the x-space using the Chebyshev-polynomial expansion and then after integrating over x we have got the prediction $q_1^{\rm CHEB}$, which can be treated as an exact one. Next, using the evolution equations written in the moment space, we have found a closed system of $m+1$ solutions for the truncated moments, where the result $q_1^{{\rm FMPR}\text{-}m}$ obtained is expressed by values of the m higher moments. The considered numbers of terms in the truncated series were $m = 4$ and $m = 30$. Working in the moment space we have also found an alternative way to determine the small-x_0 behaviour of the truncated first

moment. Taking into account the relation between the nth and jth truncated moment, we were able to derive the evolution equation, which does not contain mixing between different moments. Then, adopting the standard analytical method of the full moments to the case of the first truncated moment, we have found the approximate behaviour of q_1 as $x \to 0$. In this way the inverse Mellin transform performed with the use of the method of steepest descent implies the result q_1^{MM} within our modified "moment of moment" approach.

We have shown that for small $x_0 \leq 0.01$ there is a good agreement between the MM results and the reliable predictions, obtained with the use of the Chebyshev-polynomial method. This agreement occurs independently either on the shape of the input parametrisation or on the value of Q^2. It has been also found that for small x_0 the accuracy of the q_1^{MM} and $q_1^{\mathrm{FMPR\text{-}30}}$ results are similar, being clearly better than in the case of $q_1^{\mathrm{FMPR\text{-}4}}$ predictions.

We have presented results concerning the spin structure function g_1^{NS} and the contribution truncated at $x_0 = 0.01$ to the Bjorken sum rule. It has been found that the choice of the input parametrisation has a large impact on the evaluation of the low-x contribution to the BSR. This contribution can vary from a few percents for the flat ($\sim$ const) input to tens of percents for the steep ($\sim x^{-0.5}$) one. Recent experimental data confirm the rise of the polarised structure functions at small x. However, because of the large uncertainties, reliable support or contradiction of the theoretical expectations is still out of reach.

References

1. K. Gottfried, Phys. Rev. Lett. **18**, 1174 (1967)
2. J.D. Bjorken, Phys. Rev. **148**, 1467 (1966)
3. J.D. Bjorken, Phys. Rev. D **1**, 1376 (1970)
4. V.N. Gribov, L.N. Lipatov, Sov. J. Nucl. Phys. **15**, 438 (1972)
5. V.N. Gribov, L.N. Lipatov, Sov. J. Nucl. Phys. **15**, 675 (1972)
6. Y.L. Dokshitzer, Sov. Phys. JETP **46**, 641 (1977)
7. G. Altarelli, G. Parisi, Nucl. Phys. B **126**, 298 (1977)
8. S. Forte, L. Magnea, Phys. Lett. B **448**, 295 (1999) [hep-ph/9812479]
9. S. Forte, L. Magnea, A. Piccione, G. Ridolfi, Nucl. Phys. B **594**, 46 (2001) [hep-ph/0006273]
10. A. Piccione, Phys. Lett. B **518**, 207 (2001) [hep-ph/0107108]
11. D. Kotlorz, A. Kotlorz, Acta Phys. Pol. B **36**, 3023 (2005) [hep-ph/0510295].
12. S. Kumano, T.-H. Nagai, J. Comput. Phys. **201**, 651 (2004) [hep-ph/0405160].
13. C. Coriano, C. Savkli, Comput. Phys. Commun. **118**, 236 (1999) [hep-ph/9803336]
14. R. Kobayashi, M. Konuma, S. Kumano, M. Miyama, Prog. Theor. Phys. Suppl. **120**, 257 (1995) [hep-ph/9412341]
15. J. Kwieciński, D. Strózik-Kotlorz, Z. Phys. C **48**, 315 (1990)
16. J. Kwieciński, B. Ziaja, Phys. Rev. D **60**, 054004 (1999) [hep-ph/9902440]
17. B. Badełek, J. Kwieciński, Phys. Lett. B **418**, 229 (1988) [hep-ph/9709363]
18. J. Kwieciński, M. Maul, Phys. Rev. D **67**, 034014 (2003) [hep-ph/0111031]
19. S.E. El-gendi, Comput. J. **12**, 282 (1969)
20. A. De Rújula, S.L. Glashow, H.D. Politzer, S.B. Treiman, F. Wilczek, A. Zee, Phys. Rev. D **10**, 1649 (1974)
21. B.I. Ermolaev, M. Greco, S.I. Troyan, Nucl. Phys. B **571**, 137 (2000) [hep-ph/9906276]
22. B.I. Ermolaev, Nucl. Phys. B **594**, 71 (2001) [hep-ph/0009037]
23. Particle Data Group, S. Eidelman et al., Phys. Lett. B **592**, 1 (2004)
24. SMC Collaboration, D. Adams et al., Phys. Rev. D **56**, 5330 (1997)
25. B. Adeva et al., Phys. Lett. B **420**, 180 (1998)
26. B. Adeva et al., Phys. Rev. D **58**, 112002 (1998)
27. E154 Collaboration, K. Abe et al., Phys. Rev. Lett. **79**, 26 (1997)
28. E155 Collaboration, P.L. Anthony et al., Phys. Lett. B **463**, 339 (1999)
29. HERMES Collaboration, K. Ackerstaff et al., Phys. Lett. B **404**, 383 (1997)
30. HERMES Collaboration, K. Ackerstaff et al., Phys. Lett. B **464**, 123 (1999)
31. A. Airapetian et al., Phys. Lett. B **442**, 484 (1998)
32. HERMES Collaboration, A. Airapetian et al., Phys. Rev. D **71**, 012001 (2005) [hep-ex/0407032]
33. J. Kwieciński, Acta Phys. Pol. B **27**, 893 (1996)
34. J. Bartels, B.I. Ermolaev, M.G. Ryskin, Z. Phys. C **70**, 273 (1996)
35. J. Bartels, B.I. Ermolaev, M.G. Ryskin, Z. Phys. C **72**, 627 (1996)
36. S.D. Bass, Rev. Mod. Phys. Pol. **77**, 1257 (2005) [hep-ph/0411005]